Review

Formation of Inorganic–organic Nanohybrids through Self-assembly of Perylene Bisimide Derivatives

Norihiro Mizoshita, Takao Tani and Shinji Inagaki

Report received on Jul. 25, 2013

ABSTRACT Various types of nanostructured perylene bisimide (PBI)–silica hybrids have been developed using the self-assembling properties of PBI derivatives into columnar aggregates. A PBI-based organoalkoxysilane precursor exhibited a columnar liquid-crystalline (LC) phase. Uniaxial alignment of the LC precursor by dip-coating and subsequent in situ polycondensation resulted in highly conductive organosilica films. The formation of homogeneous LC phases was also achieved from a mixture of an amphiphilic PBI and tetramethoxysilane. The LC mixture could be macroscopically oriented by mechanical shearing, which was applied to the preparation of oriented nanoporous silica films. Surfactant-directed polycondensation of PBI precursors with four alkoxysilyl groups afforded a new class of molecularly ordered periodic mesoporous organosilicas (PMOs). The frameworks of the PMOs consisted of π–π stacking PBI–silica columns that exhibited significant optical and electronic properties. The formation of inorganic–organic nanostructures driven by strong intermolecular interactions of organic chromophores should contribute to the development of optically and electronically functional nanohybrid materials.

KEYWORDS Self-assembly, Organosilica, Perylene Bisimide, Liquid Crystals, Mesostructures, Nanoporous Materials

1. Introduction

Inorganic–organic hybrid materials have attracted much attention because such material design enables the combination of various functionalities and the induction of synergetic effects of the inorganic and organic components.[1] Silica-based hybrid materials have been particularly studied due to the ease of synthesis of the functionalized precursors, good controllability of the condensation reaction, flexibility for chemical modification, and the high chemical stability of the silica scaffold. Polycondensation of tetraalkoxysilanes in the presence of organic templates yields nanostructured materials that consist of pure silica and organic molecules.[2,3] Polycondensation of organoalkoxysilanes ($R[Si(OR')_3]_n$; R: organic group, R': Me, Et, etc.) results in covalently crosslinked organosilica hybrids, such as organosilsesquioxanes,[4,5] and periodic mesoporous organosilicas (PMOs).[6,7] In these materials, organic–organic interactions, as well as inorganic–organic interactions, play an important role in the formation of nanohybrid structures and the induction of significant optical and electronic properties.

Perylene bisimide (PBI) derivatives are a promising building block for functional nanostructured materials. The strong π-stacking nature of PBI derivatives has led to the construction of ordered molecular assemblies.[8] Moreover, the PBI unit exhibits high chemical stability,[9] significant optical behavior,[10] and electron-acceptor and -transport properties.[11] The use of PBIs in preparing inorganic–organic hybrid materials could realize the development of optically and electronically functional materials with ordered nanostructures.

In this review article, focus is placed on the formation of PBI–silica nanohybrid materials driven by the π–π stacking of PBI moieties. The 1D aggregation of PBI derivatives contributes to the induction of columnar liquid-crystalline (LC) phases that comprise alkoxysilane components, which enables long-range orientation of the resulting hybrid thin films. The π-stacking nature of PBI moieties can also be utilized to synthesize a new class of PMO with molecular-scale order.

2. Highly Conductive Organosilica Films Prepared from LC Precursor

Bridged organosilane precursors ($R[Si(OR')_3]_n$; $n \geq 2$) have been widely used to prepare optically and electronically functional organosilicas.[4-7] In many cases, polycondensation of bridged organosilane

precursors yields amorphous organosilica materials.[4,5] Molecular-scale ordering in electroactive organosilicas has been reported for microtubes and -flakes containing PBI and porphyrin, respectively.[12] However, these organosilicas exhibited relatively low electronic conductivities (in the order of 10^{-7} to 10^{-4} S cm^{-1}), probably due to the limited orientation of the organic groups within the micrometer-sized tubes and flakes. If non-hydrolyzed organosilane precursors exhibit LC behavior, then molecularly ordered hybrid materials with long-range orientation could be obtained by aligning the LC precursor films and subsequent structural fixation through polycondensation. The long-range orientation of electroactive organosilicas is expected to result in enhanced electrical properties.

Organosilane compound **1** is a PBI-bridged precursor designed to exhibit LC properties (**Fig. 1**).[13] This PBI molecule has a dumbbell-like molecular shape and can form 1D columnar aggregates with rotational displacement of the PBI cores. PBI precursor **1** exhibited a columnar LC phase in the presence of organic solvents such as tetrahydrofuran (THF) and *N,N*-dimethylformamide (DMF), as well as in the pure form. Fan-like optical textures typical of columnar phases were observed for mixtures of **1** and these organic solvents (Fig. 1).

Oriented LC films of **1** were obtained by dip-coating quartz substrates with a 5 wt% solution of **1** in DMF (**Fig. 2**(a)). Figure 2(b) shows a polarized optical micrograph of the oriented film. The columnar aggregate of **1** was confirmed to be aligned along the dip-coating direction by polarized UV-vis absorption spectroscopy. The long-range orientation of the film was retained after in situ polycondensation of **1** by exposure to vapor from aqueous NH_3 or acetic acid solutions (Fig. 2(c)). Transmission electron microscopy (TEM) observation revealed that the polycondensed films, denoted as **1**-NH_3, had striped structures with periodicities of 1–2 nm, which correspond to oriented columnar structures (Fig. 2(c), inset).

The oriented films exhibited high and anisotropic electrical conductivities in the presence of an electron dopant (hydrazine vapor). **Table 1** lists the electrical

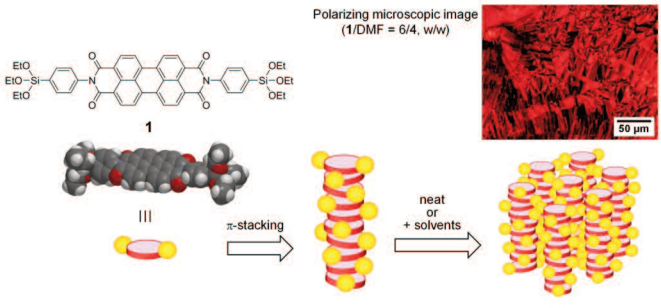

Fig. 1 Self-assembly of **1** into a columnar LC structure.

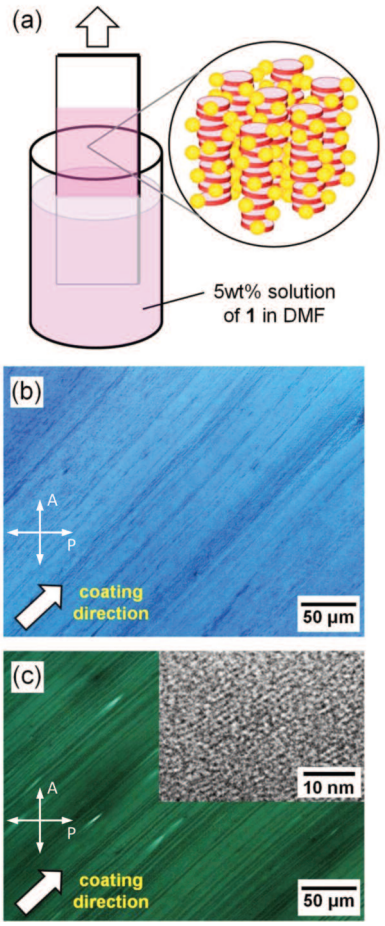

Fig. 2 (a) Schematic illustration of the preparation of oriented LC film of **1** by dip-coating. (b) Polarized optical micrograph of the oriented LC film of **1** (P: polarizer, A: analyzer). (c) Polarized optical micrograph of **1**-NH_3. The inset of (c) shows a TEM image of **1**-NH_3.

Table 1 Electrical properties of dip-coated PBI film[a] measured in saturated hydrazine vapor.

Sample	$\sigma_{\parallel}$ (S cm^{-1})	$\sigma_{\perp}$ (S cm^{-1})	$\sigma_{\parallel}/\sigma_{\perp}$
1	$(1.1 \pm 0.6) \times 10^{-1}$	$(2.7 \pm 1.3) \times 10^{-3}$	40–50
1-NH_3	$(4.4 \pm 2.2) \times 10^{-2}$	$(2.2 \pm 1.1) \times 10^{-2}$	2–3
1-AcOH	$(3.3 \pm 1.6) \times 10^{-2}$	$(6.3 \pm 3.1) \times 10^{-3}$	5–8

[a] film thickness: 7–15 nm; channel width: 4–5 mm; channel length: 150–210 μm. The measurements were conducted in nine points for each sample and averaged.

conductivities parallel ($\sigma_{\parallel}$) and perpendicular ($\sigma_{\perp}$) to the dip-coating direction of the doped films. The LC film of **1** exhibited the highest electrical conductivity, in the order of 10^{-1} S cm^{-1}, in the dip-coating direction, i.e., in the π–π stacking direction of the PBI moiety. The anisotropy of conductivity ($\sigma_{\parallel}/\sigma_{\perp}$) was greater than 40. After polycondensation, the organosilica films (**1**-NH_3 and **1**-AcOH) exhibited electrical conductivities ($\sigma_{\parallel}$) in the order of 10^{-2} S cm^{-1}. These are the highest level conductivities for organosilica materials[12,14] and are also comparable to those reported for all-organic PBI assemblies.[15] Although the columnar order of **1**-NH_3 and **1**-AcOH is slightly disturbed by polycondensation, the anisotropic alignment of the PBI moiety is retained in the silica scaffold (Fig. 2), which leads to the suppression of a large decrease in $\sigma_{\parallel}$. Thus, the use of LC organosilane precursors can realize long-range orientation of resulting organosilica hybrid films and can induce significant electrical properties.

3. Solvent-free Synthesis of Oriented PBI–silica Hybrid Films

The use of amphiphilic PBI compound **2** enables a new approach to the formation of macroscopically oriented PBI–silica hybrid and nanoporous silica films from solvent-free LC mixtures (**Fig. 3**).[16] In the conventional sol–gel synthesis of organic–silica hybrids (Fig. 3(b), left), cooperative self-assembly of organic templates and hydrolyzed precursors in the presence of solvents results in nanostructured materials. An alternative method that uses aqueous lyotropic LC phases as templates was reported by Attard and coworkers (Fig. 3(b), center).[17] In these methods, the lyotropic templates formed in the presence of a large quantity of solvent exhibit high fluidity; therefore, the preparation of uniaxially oriented materials requires deposition onto well-oriented solid substrates[18] or the application of external fields.[19] In contrast, a mixture of amphiphilic PBI derivative **2** and tetramethoxysilane (TMOS) can form homogeneous LC phases in the absence of solvents and without hydrolysis of TMOS, which facilitates long-range orientation of the precursor mixture and formation of oriented nanoporous silica film (Fig. 3(b), right).

The **2**–TMOS mixtures containing less than 40 wt% TMOS exhibited columnar LC phases. **Figure 4** shows polarized optical micrographs of the mixtures with different **2**/TMOS ratios. Compound **2** was reported to exhibit a hexagonal columnar (Col_h) phase in the pure form (Fig. 4(a)).[20] The **2**–TMOS mixtures containing less than 30 wt% TMOS maintained the Col_h phase (Fig. 4(b)). X-ray diffraction (XRD) measurements showed that the *d*-spacing values corresponding to the (100) plane of the Col_h phase increased from 1.78 to 2.11 nm with an increase of TMOS from 0 to 25 wt%, which indicates expansion of the 2D packing structure of the columns. The **2**–TMOS mixtures containing 30–40 wt% TMOS formed a nematic columnar (N_{col}) phase and exhibited schlieren texture (Fig. 4(c)). For

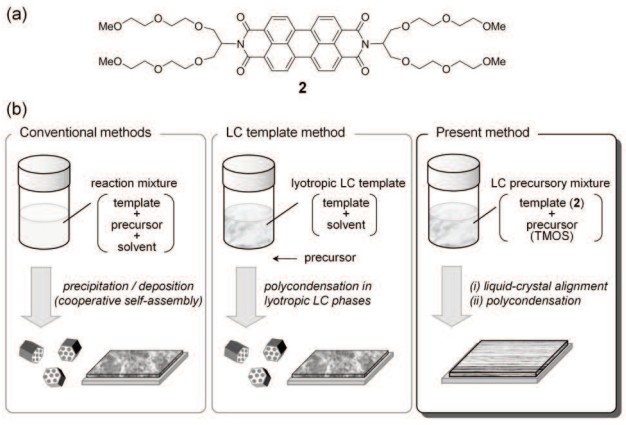

Fig. 3 (a) Chemical structure of PBI template **2**. (b) Comparison of the preparation methods for nanoporous materials from isotropic and LC sol mixtures.

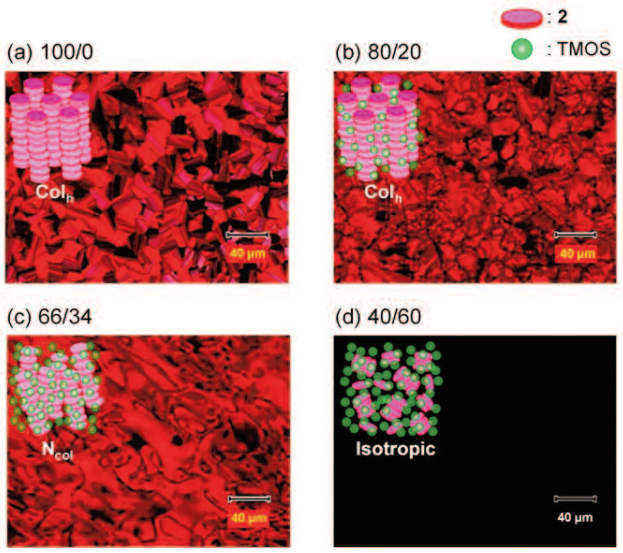

Fig. 4 Polarized optical micrographs of **2**–TMOS (w/w) mixtures.

the mixtures containing more than 50 wt% TMOS, no LC structure was observed at room temperature (Fig. 4(d)).

The **2**–TMOS (66/34, w/w) mixture containing a small amount of hydrochloric acid was mechanically sheared between glass substrates to form oriented **2**–silica hybrid films. The film exhibited a bright homogeneous texture under a polarizing microscope when the shearing direction was 45° from the polarization direction, which indicates the long-range orientation of the film (**Fig. 5**(a)). Partial condensation of TMOS effectively suppressed the fluidity of the mixture and allowed permanent shear-induced LC alignment. The columnar structure was confirmed to be oriented in the shearing direction by polarized UV-vis spectroscopy. Aging of the acid-containing mixture led to fixation of the oriented structure by the polycondensation of TMOS. The **2**–silica hybrid film exhibited an XRD peak at d = 1.84 nm, which corresponds to the intercolumnar spacing. Removal of **2** from the hybrid film resulted in an oriented nanoporous silica film (Fig. 5(b)). A macroscopically oriented silica structure was observed over the entire surface of the glass substrate. TEM observation of the calcined material revealed the formation of an oriented nanoporous structure with a periodicity of ca. 2 nm. Although the nanoscale periodicity of the silica framework is disturbed after the removal of **2**, due to the small proportion of TMOS in the LC precursor mixture, this solvent-free approach enables the facile preparation of macroscopically oriented nanohybrid and nanoporous materials without any specific pretreatment of the substrates. Various hybrid materials with long-range orientation could be developed by extending the combination of precursors and templates that exhibit homogeneous LC phases.

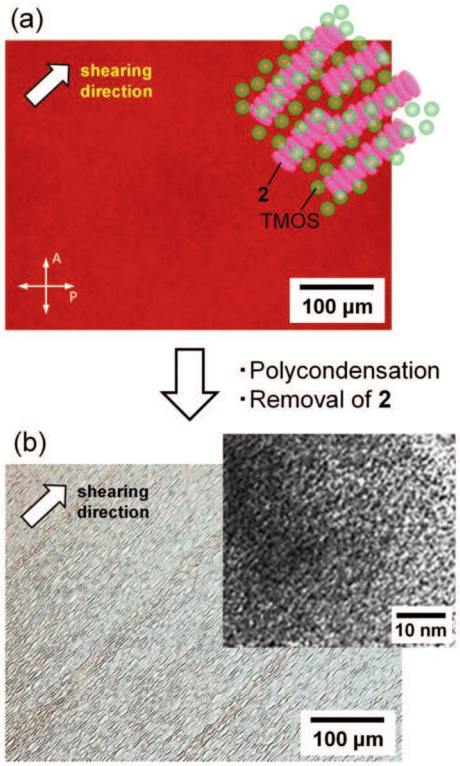

Fig. 5 (a) Polarized optical micrograph of the oriented **2**–TMOS (66/34, w/w) mixture containing a small amount of hydrochloric acid. (b) Optical micrograph of the oriented nanoporous silica film after washing with chloroform. The inset of (b) shows a TEM image of the nanoporous silica film after calcination.

4. PMO with π-Stacked Framework

A large number of PMOs have been prepared by surfactant-directed polycondensation of bridged organosilane precursors.[6,7] One breakthrough in the research of PMOs is the induction of molecular-scale periodicity in the framework.[6,7,21] Frameworks of PMOs with specific bridging groups, such as 1,4-phenylene, 4,4'-biphenylylene, and 2,6-naphthylene, can form "crystal-like" layered structures (**Fig. 6**(a), left). However, the distance between the neighboring organic bridges (ca. 0.44 nm) in such configurations is much longer than the typical face-to-face π–π stacking distance (0.34–0.36 nm). If aromatic organic groups are densely packed with π–π stacking distances within the framework of PMO, then strong electronic coupling and significant electroconductive properties can be expected for the pore walls (Fig. 6(a), right).

A new class of molecularly ordered PMOs with π–π stacking columns were developed using PBI derivatives **3** with four alkoxysilyl groups (Fig. 6(b)).[22] The formation of the new nanohybrid structure was realized by the cooperative effect of columnar self-assembly of the disk-like precursors and electrostatic interaction between a cationic surfactant and the silanolate groups of the PBI aggregates (Fig. 6(c)). The organosilica framework was reinforced with a pure silica coating to avoid collapse of the periodic mesostructure by removal of the surfactant template. PBI-based PMOs (**3a**-PMO and **3b**-PMO) were obtained by washing the silica-reinforced materials with ethanol. **Figure 7**(a) shows an XRD pattern of **3a**-PMO. The intense peak at d = 4.02 nm corresponds to the periodicity of the mesoporous

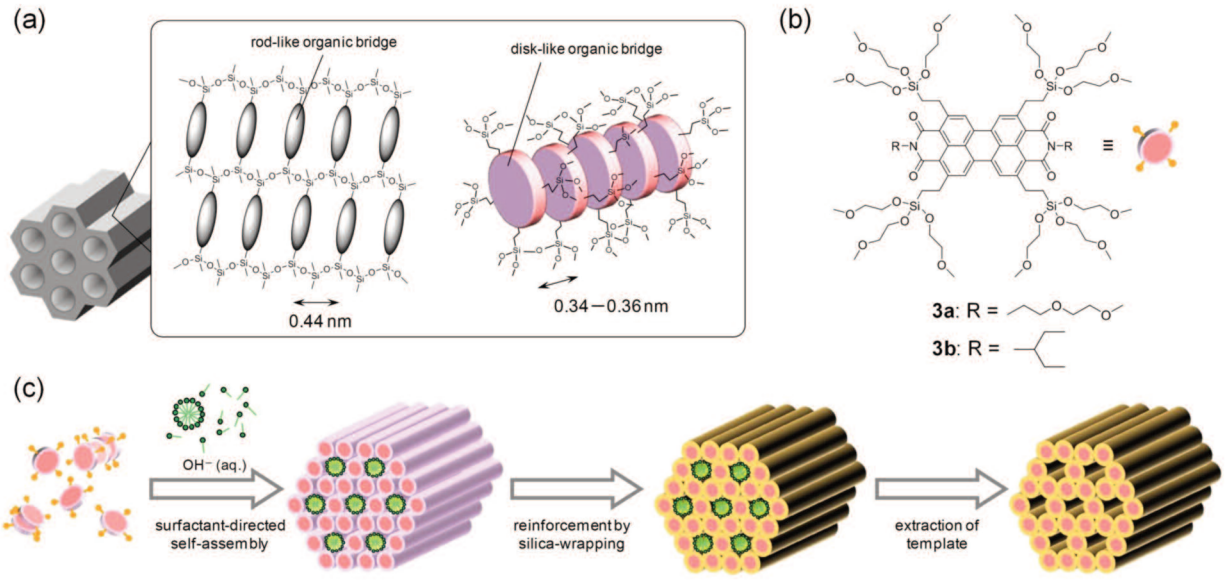

Fig. 6 (a) Illustration of molecularly ordered organosilica frameworks of PMOs with rod-like (left) and disk-like (right) organic bridges. (b) Chemical structures of the PBI-derived precursors. (c) Preparation of PMO hybrids from disk-like PBI precursors.

structure and the π–π stacking periodicity within the pore wall was observed at d = 0.35 nm. **3b**-PMO had a similar XRD pattern. The Brunauer–Emmett–Teller (BET) surface area, pore volume, and pore diameter were calculated from nitrogen adsorption–desorption isotherms to be 609 $m^2\ g^{-1}$, 0.25 $cm^3\ g^{-1}$, and 2.6 nm for **3a**-PMO and 663 $m^2\ g^{-1}$, 0.29 $cm^3\ g^{-1}$, and 2.6 nm for **3b**-PMO, respectively. The formation of a mesochannel array was also confirmed by TEM observation (Fig. 7(b)).

The π-stacked PBI–silica framework exhibited significant optical and electronic properties. **Table 2** summarizes the π-stacking periodicity, absorption maximum wavelength (λ_{abs}), and electronic properties of the **3**-PMOs and related materials. Although **3a**-PMO and **3b**-PMO have a similar π-stacking periodicity, the λ_{abs} of **3a**-PMO is much shorter than those of **3b**-PMO, the amorphous PBI–silica synthesized from **3b** (**3b**-Amorph), and a solution of **3a** in THF. The hypsochromic shift of λ_{abs} for **3a**-PMO indicates close face-to-face stacking and exciton coupling of the PBI chromophores. In contrast, the exciton coupling among the PBI chromophores of **3b**-PMO is weak or absent, which suggests that the PBI moieties form π–π stacking structures, but with orthogonal transition dipole moments (i.e., molecular axes). Compared to **3a**-PMO with a short linear substituent on the imide groups, the bulky 3-pentyl substituent of **3b**-PMO is likely to promote orthogonal arrangement of the PBI moieties to avoid steric hindrance. The PBI-bridged PMOs also exhibited

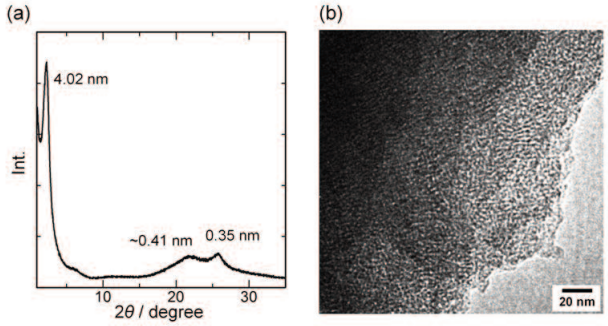

Fig. 7 (a) XRD pattern and (b) TEM image of **3a**-PMO.

Table 2 Structural, optical, and electronic properties of **3**-PMOs, **3b**-Amorph, and a solution of **3a**.

Sample	π-stacking periodicity (nm)	λ_{abs} (nm)	Concentration of radical spin (mol%)[a]	ΔH_{pp} (G)[a]
3a-PMO	0.35	498	0.42	4.9
3b-PMO	0.36	529	0.27	7.0
3b-Amorph	–	526	not detected	–
3a (in solution)	–	521[b]	–	4.4[c]

[a] ESR measurements of PBI–silica hybrids were conducted in saturated hydrazine vapor for electron doping at room temperature.
[b] Measured in THF.
[c] Measured in THF/DMF/hydrazine (5/1/1, v/v/v).

different electron-accepting properties. When the PMOs and **3b**-Amorph were exposed to saturated hydrazine vapor for electron doping, the concentrations of resulting PBI anionic radicals, which were calculated from electron spin-resonance (ESR) spectra, were in the order **3a**-PMO > **3b**-PMO >> **3b**-Amorph (Table 2). This result indicates that π-stacked PBI assemblies exhibiting strong exciton coupling are advantageous for electron doping. Although the peak-to-peak linewidth (ΔH_{pp}) of the ESR spectra for the PMOs was apt to increase in comparison with a solution of the precursor, due to inhomogeneity of the powder samples, ΔH_{pp} for **3a**-PMO was significantly smaller than that for **3b**-PMO. This implies hopping or delocalization of the unpaired electron over several PBI sites in **3a**-PMO.[23] The PMOs with π-stacked frameworks have significant potential for the design of functional hybrid materials, such as solid-state catalysts and high-performance electronic devices.

5. Conclusions

A variety of nanostructured PBI–silica hybrid materials were synthesized by utilizing the columnar self-assembly of PBI derivatives. The formation of LC phases comprising non-hydrolyzed precursors was the key to macroscopically align the resulting PBI–silica hybrid films. Surfactant-directed self-assembly of the PBI-derived precursors resulted in a new class of PMOs with π-stacked frameworks. This synthesis strategy exploits the strong interactions of organic chromophores and is applicable to the development of photofunctional and electroactive nanohybrids.

Acknowledgements

This report is based on original papers referenced from *Advanced Functional Materials*,[13] *Chemical Communications*,[16] and *Angewandte Chemie International Edition*.[22] Table 1 was adapted from Ref. 13 with permission from Wiley-VCH Verlag GmbH & Co. KGaA. Figure 3 was adapted from Ref. 16 with permission from The Royal Society of Chemistry. Figure 6 was adapted from Ref. 22 with permission from Wiley-VCH Verlag GmbH & Co. KGaA. In the adapted materials, the sample names were adjusted to those used in the present manuscript. The authors thank Prof. Hiroshi Shinokubo of Nagoya University for helpful discussions.

References

(1) Descalzo, A. B., Martínez-Máñez, R., Sancenón, F., Hoffmann, K. and Rurack, K., *Angew. Chem. Int. Ed.*, Vol. 45, No. 36 (2006), pp. 5924-5948.
(2) Ying, J. Y., Mehnert, C. P. and Wong, M. S., *Angew. Chem. Int. Ed.*, Vol. 38, No. 1-2 (1999), pp. 56-77.
(3) Kresge, C. T., Leonowicz, M. E., Roth, W. J., Vartuli, J. C. and Beck, J. S., *Nature*, Vol. 359, No. 6397 (1992), pp. 710-712.
(4) Corriu, R. J. P., *Angew. Chem. Int. Ed.*, Vol. 39, No. 8 (2000), pp. 1376-1398.
(5) Shea, K. J. and Loy, D. A., *Chem. Mater.*, Vol. 13, No. 10 (2001), pp. 3306-3319.
(6) Mizoshita, N., Tani, T. and Inagaki, S., *Chem. Soc. Rev.*, Vol. 40, No. 2 (2011), pp. 789-800.
(7) Wang, W., Lofgreen, J. E. and Ozin, G. A., *Small*, Vol. 6, No. 23 (2010), pp. 2634-2642.
(8) (a) Würthner, F., *Chem. Commun.*, No. 14 (2004), pp. 1564-1579: (b) Görl, D, Zhang, X. and Würthner, F., *Angew. Chem. Int. Ed.*, Vol. 51, No. 26 (2012), pp. 6328-6348.
(9) Peneva, K., Mihov, G., Herrmann, A., Zarrabi, N., Börsch, M., Duncan, T. M. and Müllen, K., *J. Am. Chem. Soc.*, Vol. 130, No. 16 (2008), pp. 5398-5399.
(10) (a) Wang, H., Kaiser, T. E., Uemura, S. and Würthner, F., *Chem. Commun.*, No. 10 (2008), pp. 1181-1183: (b) Kaiser, T. E., Wang, H., Stepanenko, V. and Würthner, F., *Angew. Chem. Int. Ed.*, Vol. 46, No. 29 (2007), pp. 5541-5544.
(11) Li, C. and Wonneberger, H., *Adv. Mater.*, Vol. 24, No. 5 (2012), pp. 613-636.
(12) (a) Yang, L., Peng, H., Huang, K., Mague, J. T., Li, H. and Lu, Y., *Adv. Funct. Mater.*, Vol. 18, No. 10 (2008), pp. 1526-1535: (b) Peng, H. and Lu, Y., *Adv. Mater.*, Vol. 20, No. 4 (2008), pp. 797-800.
(13) Mizoshita, N., Tani, T. and Inagaki, S., *Adv. Funct. Mater.*, Vol. 21, No. 17 (2011), pp. 3291-3296.
(14) Imae, I., Takayama, S., Tokita, D., Ooyama, Y., Komaguchi, K., Ohshita, J., Sugioka, T., Kanehira, K. and Harima, Y., *Polymer*, Vol. 50, No. 26 (2009), pp. 6198-6201.
(15) (a) Che, Y., Datar, A., Yang, X., Naddo, T., Zhao, J. and Zang, L., *J. Am. Chem. Soc.*, Vol. 129, No. 20 (2007), pp. 6354-6355: (b) Gregg, B. A. and Cormier, R. A., *J. Am. Chem. Soc.*, Vol. 123, No. 32 (2001), pp. 7959-7960.
(16) Mizoshita, N., Tani, T. and Inagaki, S., *Chem. Commun.*, Vol. 48, No. 87 (2012), pp. 10772-10774.
(17) Attard, G. S., Glyde, J. C. and Göltner, C. G., *Nature*, Vol. 378, No. 6555 (1995), pp. 366-368.
(18) (a) Miyata, H., Kawashima, Y., Itoh, M. and Watanabe, M., *Chem. Mater.*, Vol. 17, No. 21 (2005), pp. 5323-5327: (b) Fukumoto, H., Nagano, S., Kawatsuki, N. and Seki, T., *Chem. Mater.*, Vol. 18, No. 5 (2006), pp. 1226-1234: (c) Suzuki, T., Kanno, Y., Morioka, Y. and Kuroda, K., *Chem. Commun.*, No. 28 (2008), pp. 3284-3286:

(d) Hara, M., Nagano, S. and Seki, T., *J. Am. Chem. Soc.*, Vol. 132, No. 39 (2010), pp. 13654-13656.
(19) Yamauchi, Y., Sawada, M., Noma, T., Ito, H., Furumi, S., Sakka, Y. and Kuroda, K., *J. Mater. Chem.*, Vol. 15, No. 11 (2005), pp. 1137-1140.
(20) Wicklein, A., Lang, A., Muth, M. and Thelakkat, M., *J. Am. Chem. Soc.*, Vol. 131, No. 40 (2009), pp. 14442-14453.
(21) Inagaki, S., Guan, S., Ohsuna, T. and Terasaki, O., *Nature*, Vol. 416, No. 6878 (2002), pp. 304-307.
(22) Mizoshita, N., Tani, T., Shinokubo, H. and Inagaki, S., *Angew. Chem. Int. Ed.*, Vol. 51, No. 5 (2012), pp. 1156-1160.
(23) (a) Wilson, T. M., Zeidan, T. A., Hariharan, M., Lewis, F. D. and Wasielewski, M. R., *Angew. Chem. Int. Ed.*, Vol. 49. No. 13 (2010), pp. 2385-2388: (b) Chen, S.-G., Branz, H. M., Eaton, S. S., Taylor, P. C., Cormier, R. A. and Gregg, B. A., *J. Phys. Chem. B*, Vol. 108, No. 45 (2004), pp. 17329-17336.

Norihiro Mizoshita
Research Field:
- Synthesis and Functionalization of Organosilica Hybrid Materials

Academic Degree: Ph.D.
Academic Societies:
- The Chemical Society of Japan
- The Society of Polymer Science, Japan
- Japanese Liquid Crystal Society

Awards:
- Japanese Liquid Crystal Society Paper Award (A), 2000
- Young Scientist Award of Japanese Liquid Crystal Society, 2006

Takao Tani
Research Fields:
- Functionalization of Periodic Mesoporous Organosilicas
- Flame Synthesis of Metal Oxide Nanoparticles and Their Applications

Academic Degree: Dr. sc. techn. ETH
Academic Societies:
- The Ceramic Society of Japan
- The Japanese Sol-Gel Society

Award:
- 40th Tokai Chemical Industry Association Award, 2005

Shinji Inagaki
Research Field:
- Synthesis and Applications of Mesoporous Materials

Academic Degree: Ph.D.
Academic Societies:
- The Chemical Society of Japan
- Catalysis Society of Japan
- Japan Association of Zeolite
- The Japan Society on Adsorption
- The Society of Polymer Science, Japan
- International Mesostructured Materials Association
- International Zeolite Association

Awards:
- The Award of Chemistry on Catalyst Preparation, 1994
- The Promotion Award of the Japan Society on Adsorption, 2001
- The Chemical Society of Japan Award for Creative Work, 2004
- The Minister Award of Education, Culture, Sport, Science and Technology, 2005
- The Japan Society on Adsorption Award, 2008

